J|A|C|S ARTICLES

Published on Web 02/10/2010

The Crystalline Nanocluster Phase as a Medium for Structural and Spectroscopic Studies of Light Absorption of Photosensitizer Dyes on Semiconductor Surfaces

Jason B. Benedict* and Philip Coppens*

Department of Chemistry, University at Buffalo, State University of New York, Buffalo, New York 14260-3000

Received November 11, 2009; E-mail: coppens@buffalo.edu

Abstract: The crystalline nanocluster phase, in which nanoscale metal oxide clusters are self-assembled in three-dimensional periodic arrays, is described. The crystalline assembly of nanoparticles functionalized with technologically relevant ligands offers the opportunity to obtain unambiguous structural information that can be combined with theoretical calculations based on the known geometry and used to interpret spectroscopic and other information. A series of Ti/O clusters up to ~2.0 nm in diameter have been synthesized and functionalized with the adsorbents catechol and isonicotinic acid. Whereas the isonicotinate is always adsorbed in a bridging monodentate mode, four different adsorption modes of catechol have been identified. The particles show a significantly larger variation of the Ti−O distances than observed in the known TiO_2 phases and exhibit both sevenfold overcoordination and five- and fourfold undercoordination of the Ti atoms. Theoretical calculations show only a moderate dependence of the catecholate net charge on the geometry of adsorption. All of the catechol-functionalized clusters have a deep-red color due to penetration of the highest occupied catechol levels into the band gap of the Ti/O particles. Spectroscopic measurements of the band gap of the Ti_{17} cluster are in good agreement with the theoretical values and show a blue shift of ~0.22 eV relative to those reported for anatase nanoparticles.

Introduction

Semiconductor surfaces are key components of molecule-based photovoltaic cells, and TiO_2 surfaces in particular have therefore received extensive attention.[1] A series of theoretical calculations on titanium oxide particle/molecular adsorbent complexes have been reported,[2−5] but detailed diffraction information on the structure of the photosensitizer−semiconductor surface is not available. It has not been generally recognized that a number of crystalline materials are known in which nanoscale metal oxide clusters are aligned in periodic arrays (see Figure 1), the structure of which can be determined accurately by diffraction methods. TiO_2 cluster phases have been studied because of their catalytic properties,[6] such as in the photoreduction of CO_2 to methane and methanol and in esterification and polymerization reactions, as well as their use as precursors in the synthesis of metal oxide ceramics. A number of structure determinations have been reported. Corden and co-workers synthesized di-, tri-, and pentanuclear titanium species and examined their catalytic activities in esterification reactions.[7] Sanchez and co-workers synthesized the cluster $[Ti_{17}O_{24}(OPr^i)_{20}]$;[8] this species and the clusters $[Ti_{18}O_{28}H(OBu^t)_{17}])$ and $([Ti_{18}O_{22}(OBu^n)_{26}(acac)_2]$[9] are the largest Ti/O clusters reported in the literature.

The work described here was specifically aimed at examining the properties of the nanoclusters as models for TiO_2 surfaces across which electron injection takes place in photovoltaic cells. After a description of the synthetic methods, we discuss the experimentally determined structures, their comparison with known TiO_2 phases, the geometry of adsorption of dye molecules, their spectroscopic properties, and the nature of the bonding as revealed by the experimental results and parallel theoretical calculations based on the experimental geometry.

Experimental Section

Synthetic Strategies. Two synthetic strategies were employed. In the first, new clusters were synthesized using a monomeric titanium alkoxide precursor either with or without a photosensitizer dye such as catechol (cat-H_2, pyrocatechol) or pyridyl-4-carboxylic acid (isonicotinic acid, INA) added to the reaction mixture. Progressively larger clusters with $n_{Ti} = 2$, 3, 4, 6, and 17 Ti atoms were obtained by increasing the temperature at which the reaction

(1) Diebold, U. *Surf. Sci. Rep.* **2003**, *48*, 53–229.
(2) Duncan, W. R.; Prezhdo, O. V. *Annu. Rev. Phys. Chem.* **2007**, *58*, 143–184.
(3) Persson, P.; Ojamae, L. *Chem. Phys. Lett.* **2000**, *321*, 302–308. Persson, P.; Lundqvist, M. J. *J. Phys. Chem. B* **2005**, *109*, 11918–11924.
(4) Lundqvist, M. J.; Nilsing, M.; Lunell, S.; Åkermark, B.; Persson, P. *J. Phys. Chem. B* **2006**, *110*, 20513–20525.
(5) Lundqvist, M. J.; Nilsing, M.; Persson, P.; Lunell, S. *Int. J. Quantum Chem.* **2006**, *106*, 3214–3234.
(6) Li, G.; Dimitrijevic, N. M.; Chen, L.; Nichols, J. M.; Rajh, T.; Gray, K. A. *J. Am. Chem. Soc.* **2008**, *130*, 5402–5403.
(7) Corden, J. P.; Errington, W.; Moore, P.; Partridge, M. G.; Wallbridge, M. G. H. *Dalton Trans.* **2004**, 1846–1851.
(8) Steunou, N.; Kickelbick, G.; Boubekeur, K.; Sanchez, C. *J. Chem. Soc., Dalton Trans.* **1999**, 3653–3655. Steunou, N.; Portal, R.; Sanchez, C. *High Pressure Res.* **2001**, 63–70.
(9) Campana, C. F.; Chen, Y.; Day, V. W.; Klemperer, W. G.; Sparks, R. A. *J. Chem. Soc., Dalton Trans.* **1996**, 691–702. Toledano, P.; In, M.; Sanchez, C. *C. R. Acad. Sci. Paris, Ser. II* **1991**, *313*, 1247.

10.1021/ja909600w

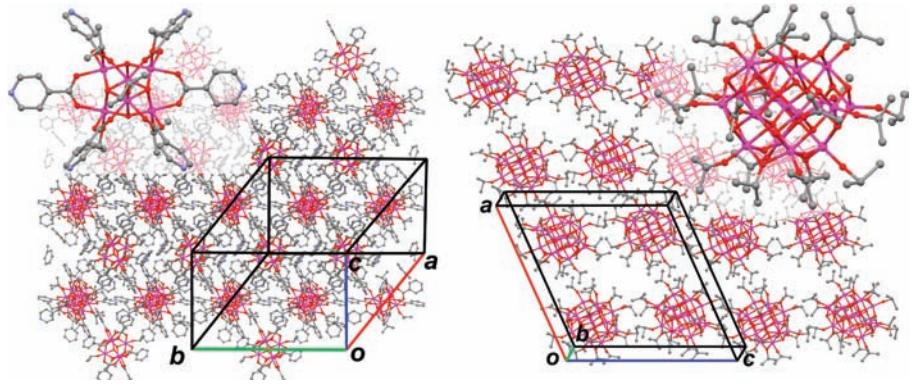

Figure 1. Periodic arrangement of the nanoclusters in crystals of (left) $\mathbf{Ti_6cat_6}$ and (right) $\mathbf{Ti_{17}}$, with the structures of individual molecules (insets). Ti, purple; O, red; C, gray; N, blue.

was carried out. In the second approach, larger bare titanium alkoxide clusters with $n_{Ti} = 17$ were reacted with the selected adsorbent molecules.

Chemicals. All of the reagents and solvents were purchased from commercial sources and used without further purification: $Ti(OPr^i)_4$ (Sigma-Aldrich), toluene (EMD), hexane (Aldrich), heptane (J. T. Baker), benzene (Aldrich), isopropyl alcohol (Fisher), pyrocatechol (Eastman Organic Chemicals), and isonicotinic acid (Alfa Aesar).

Syntheses. Reactions and recrystallizations of the titanium compounds were carried out under an argon atmosphere using standard drybox or Schlenk techniques.

$Ti_2(cat)_2(OPr^i)_4(HOPr^i)_2$ [Ti_2cat_2]. Recrystallization of 2 mL of the sticky residue formed in the $\mathbf{Ti_6cat_6}$ reaction (see below) from isopropanol yielded several small pale-red crystals of $\mathbf{Ti_2cat_2}$ suitable for structure determination.

$Ti_2(cat)_2(cat\text{-}H)_4$ [Ti_2cat_6]. To a 250 mL Schlenk flask containing a magnetic stir bar were added pyrocatechol (1.20 g, 10.9 mmol) and toluene (30 mL). The flask was then sealed with a rubber septum, pumped and purged with argon (three cycles), and placed in a room-temperature oil bath with stirring. The initially colorless solution turned dark-red when $Ti(OPr^i)_4$ (1.0 mL, 3.63 mmol) was added dropwise via syringe. After the solution was heated to 100 °C for 48 h, approximately two-thirds of the solvent was removed in vacuo. The flask was then transferred to the drybox, after which the remainder of the solvent was removed by slow evaporation, yielding a red powder and red crystals of $\mathbf{Ti_2cat_6}$ suitable for structure determination.

$Ti_3(\mu_3\text{-}O)(INA)_3(OPr^i)_7$. [$Ti_3INA_3$]. To a 250 mL Schlenk flask containing a magnetic stir bar were added INA (0.447 g, 3.63 mmol) and toluene (30 mL). The flask was then sealed with a rubber septum, pumped and purged with argon (three cycles), and placed in a room-temperature oil bath with stirring. The initially cloudy solution clarified when $Ti(OPr^i)_4$ (1.0 mL, 3.63 mmol) was added dropwise via syringe. After the solution was heated to 60 °C for 12 h, ~60% of the solvent was removed in vacuo. The flask was then transferred to the drybox, where the pale-yellow solution was allowed to slowly evaporate, yielding colorless crystals of $\mathbf{Ti_3INA_3}$ suitable for structure determination.

$Ti_4(\mu_4\text{-}O)(\mu_2\text{-}O)(INA)_2(OEt)_{10}$ [Ti_4INA_2]. To a 250 mL Schlenk flask containing a magnetic stir bar were added INA (0.447 g, 3.63 mmol) and ethanol (30 mL). The flask was then sealed with a rubber septum, pumped and purged with argon (three cycles), and placed in a room-temperature oil bath with stirring. The initially cloudy solution clarified when $Ti(OPr^i)_4$ (1.0 mL, 3.63 mmol) was added dropwise via syringe. After the solution was heated to 60 °C for 12 h, the solvent was removed in vacuo. The flask was then transferred to the drybox, where 10 mL of toluene was added to the residue. This solution was filtered. Following slow evaporation of the solvent, colorless crystals of $\mathbf{Ti_4INA_2}$ suitable for structure determination were obtained.

$Ti_6(\mu_3\text{-}O)_6(INA)_6(OPr^i)_6$ [Ti_6INA_6]. The procedure was identical to that for $\mathbf{Ti_3INA_3}$, except that the reaction was carried out at 100 °C.

$Ti_6(\mu_4\text{-}O)(cat)_6(OPr^i)_{10}\cdot$toluene [$Ti_6cat_6$]. To a 250 mL Schlenk flask containing a magnetic stir bar were added pyrocatechol (0.400 g, 3.63 mmol) and toluene (30 mL). The flask was then sealed with a rubber septum, pumped and purged with argon (three cycles), and placed in a room-temperature oil bath with stirring. The initially colorless solution became dark-red when $Ti(OPr^i)_4$ (1.0 mL, 3.63 mmol) was added dropwise via syringe. After the solution was heated to 100 °C for 48 h, the solvent was removed in vacuo. The flask was then transferred to the drybox, where the sticky red residue was redissolved in toluene. Slow evaporation of the solvent yielded red crystals of $\mathbf{Ti_6cat_6}$ suitable for structure determination.

$Ti_{17}(\mu_4\text{-}O)_4(\mu_3\text{-}O)_{16}(\mu_2\text{-}O)_4(OPr^i)_{20}$ [Ti_{17}].[8] In air, $Ti(OPr^i)_4$ (8.4 mL, 29 mmol) was quickly added via syringe to acetic acid (2.1 mL, 37 mmol) in a Teflon-lined Parr bomb with a 23 mL capacity. The bomb was sealed, placed in a 150 °C oven for 5 days, and then cooled to room temperature, after which the bomb was opened and the solution was quickly transferred by pipet to a Schlenk flask. Colorless crystals of $\mathbf{Ti_{17}}$ precipitated immediately. The atmosphere was replaced with Ar in several pump−purge cycles. This compound was identical to the one described previously by Sanchez and co-workers.[8]

$Ti_{17}(\mu_4\text{-}O)_4(\mu_3\text{-}O)_{16}(\mu_2\text{-}O)_4(INA)_4(OPr^i)_{16}$ [$Ti_{17}INA_4$]. INA (2.9 mg, 23.6 μmol) was partially dissolved in 3 mL of toluene in a small glass vial. To this was added dropwise a solution of $\mathbf{Ti_{17}}$ (14.2 mg, 5.97 μmol) in 3 mL of toluene. Slow evaporation of the dark-red solution yielded colorless crystals of $\mathbf{Ti_{17}INA_4}$ suitable for structure determination.

$Ti_{17}(\mu_4\text{-}O)_4(\mu_3\text{-}O)_{16}(\mu_2\text{-}O)_4(cat)_4(OPr^i)_{16}$ [$Ti_{17}cat_4$]. In a small glass vial, $\mathbf{Ti_{17}}$ (18.4 mg, 7.73 μmol) was dissolved in 3 mL of toluene. To this was added dropwise a solution of pyrocatechol (3.4 mg, 30.8 μmol) in 3 mL of toluene. Slow evaporation of the dark-red solution yielded red crystals of $\mathbf{Ti_{17}cat_4}$ suitable for structure determination.

Data Collection. X-ray diffraction data were collected on a Bruker SMART APEX2 CCD diffractometer installed at a rotating anode source (Mo Kα, $\lambda = 0.71073$ Å) and equipped with an Oxford Cryosystems nitrogen gas flow apparatus. In general, data were collected at 90 K, but in a few cases, higher temperatures were required because of crystal disintegration upon cooling. The oscillation method (ω scans, 180° per scan, 0.5° per frame) was used for data collection. The crystallographic data are summarized in Table S1 in the Supporting Information.

Results and Discussion

Structure. Figure 1 illustrates two examples of the periodic nature of the cluster phases, while the polyhedral building blocks of the small clusters with adsorbed catechol and INA adsorbents are shown in Figure 2.

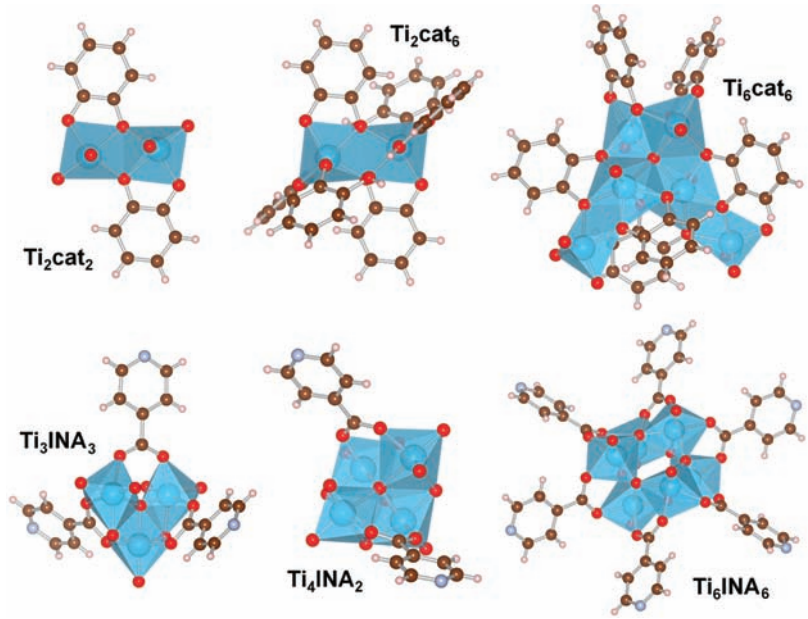

Figure 2. Views of the structures of small isolated titanium complexes with catechol and isonicotinate adsorbents, showing the polyhedral building blocks (isopropyl groups have been omitted for clarity).

Comparison of the Cluster Structures with the Pure TiO_2 Polymorphs. The three most common crystalline phases of titanium dioxide are rutile ($P4_2/mnm$, $a = b = 4.584$ Å, $c = 2.953$ Å),[10] anatase ($I4_1/amd$, $a = b = 3.782$ Å, $c = 9.502$ Å),[11] and brookite ($Pbca$, $a = 5.436$ Å, $b = 9.166$ Å, $c = 5.135$ Å).[12] In all three structures, titanium is coordinated to six oxygen atoms, forming a distorted octahedron. In the structure of rutile, the octahedron is elongated, with axial and equatorial bond lengths of 1.988 and 1.944 Å, respectively, and shares two opposing equatorial edges with neighbors. In anatase, the corresponding Ti−O bond lengths are similar at 1.980 and 1.934 Å; however, the octahedra share two pairs of two adjacent edges with neighboring octahedra. The brookite structure is strongly distorted, with the lengths of bonds trans to each other equal to 2.040 and 1.865 Å, 1.993 and 1.919 Å, and 1.993 and 1.946 Å, with corresponding distortions in the bond angles. Three of the 12 edges of each octahedron are shared between two octahedra, with two of the edges adjacent to each other. In all three structures, the individual oxygen atoms are coordinated to three different titanium atoms (μ_3-O).

The Ti/O cores of the nanoclusters share some structural similarities with the pure-phase titanium dioxide crystal structures, such as common (but not exclusive) sixfold coordination of the titanium atoms and the presence of μ_3-O bridges. However, the clusters also possess structural features absent in the bulk pure-phase crystals, such as undercoordination and overcoordination of titanium (the latter found in **Ti_6cat_6**), which are likely typical for the surfaces of the TiO_2 phases. Li et al.[6] attributed the increased reactivity of nanocluster crystals to the existence of tetrahedral Ti^{4+} sites, described as "catalytic hot spots". In the clusters examined here, four-, five-, and sevenfold coordination of titanium occurs in addition to the more common sixfold coordination. Not surprisingly, the clusters show a much larger variation of the Ti−O bond lengths and octahedral edge sharing than the pure titanium dioxide phases. The Ti−O bond lengths vary between 1.75 and 2.30 Å, compared with values of 1.934 and 1.980 Å in anatase, for example. As described above, the variation is larger in brookite, which has a much less regular structure, but is still less than that observed in the clusters. Details of the octahedral packing are dependent on the adsorbed species, as is clear from a comparison of the catechol and isonicotinate adducts of the $n_{Ti} = 6$ clusters (Figure 2). The distorted octahedra of the $n_{Ti} = 2$, 3, 4, and 6 (INA^- only) clusters lack clear axial and equatorial directions in the octahedra and most strongly resemble the distorted structure of brookite.

The Ti_{17} core has a four-coordinate titanium at its center that is surrounded by 12 six-coordinate and four five-coordinate titanium centers (the surrounding titanium polyhedra are colored blue and green, respectively, in the left column of Figure 3). Upon reaction of **Ti_{17}** with catechol and INA, the five-coordinate centers are converted to six-coordinate centers (Figure 3). In the reaction with catechol, isopropoxide groups attached to five-coordinate Ti atoms are exchanged for bidentate catechols, forming six-coordinate Ti atoms, in agreement with the change in coordination upon binding of ascorbic acid observed in XANES studies.[13] In the reaction with INA, one oxygen of the isonicotinate anion binds to the five-coordinate site, resulting in sixfold coordination, and the remaining oxygen displaces an isopropoxide group on a neighboring titanium. Following functionalization, both Ti_{17} clusters still possess a four-coordinate titanium core, but the 16 surrounding titanium atoms now all exhibit sixfold coordination. Unlike the products obtained in the synthesis of the $n_{Ti} = 6$ clusters in the presence of INA and catechol, variation of the ligand of the Ti_{17} cluster preserves the TiO core, which is identical for the two adsorbents.

The diameter of the metal oxide core of the Ti_{17} cluster is ~1.2 nm and increases to ~1.5 nm when all of the isopropoxide groups are included. The diameters of the clusters functionalized with catechol and INA are 2.0 and 1.8 nm, respectively.

(10) Baur, W. H.; Khan, A. A. *Acta Crystallogr.* **1971**, *B27*, 2133–2139.
(11) Horn, M.; Schwertfeger, C. F.; Meagher, E. P. *Z. Kristallogr.* **1972**, *136*, 273–281.
(12) Baur, W. H. *Acta Crystallogr.* **1961**, *A14*, 214–216.
(13) Rajh, T.; Nedeljkovic, J. M.; Chen, L. X.; Poluektov, O.; Thurnauer, M. C. *J. Phys. Chem. B* **1999**, *103*, 3515–3519.

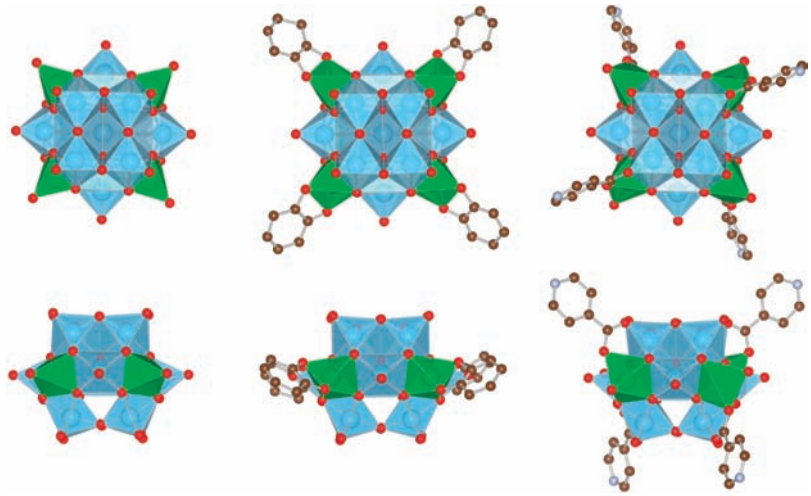

Figure 3. View parallel (upper row) and perpendicular (lower row) to the crystallographic or local S_4 axis of the semiconductor core of the bare Ti_{17} cluster (left) and the clusters functionalized with catechol (center) and INA (right). Isopropyl groups and hydrogen atoms have been omitted for clarity. Both ligands always attach to five-coordinate titanium atoms of the bare complex, resulting in the increase to sixfold coordination of the titanium atom (highlighted in green).

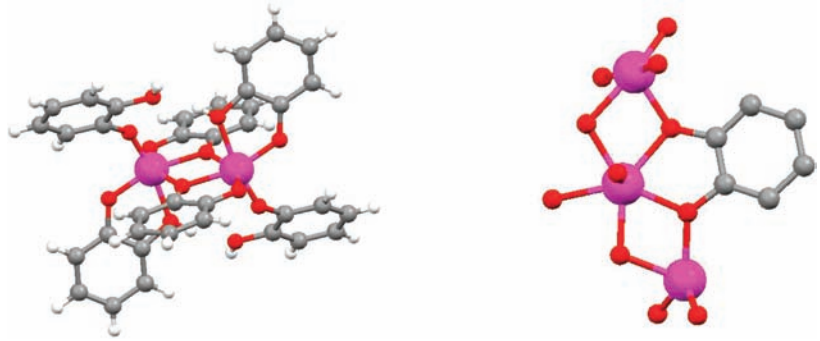

Figure 4. Different binding modes of the catecholate ion: (left) **Ti_2cat_6** showing monodentate, bidentate, and μ_2-(O,O′,O′) binding; (right) fragment of **Ti_6cat_6** showing μ_3-(O,O′,O,O′) binding.

Geometry of Adsorption. Previous theoretical calculations have shown that the manner in which a dye sensitizer binds to the substrate significantly affects the electronic properties of the system.[14] The prototypical sensitizer in photovoltaic devices is *cis*-dithiocyanatobis(2,2′-bipyridyl-4,4′-dicarboxylic acid)ruthenium(II) (N3).[15] There is a general consensus that it binds to the semiconductor substrate through the bis(isonicotinic acid) group, but geometric details of this interaction are not available. In the current work, we examined two adsorbents, catechol and INA, the latter of which is part of the adhering group of N3.

Catechol. While 19 crystal structures containing catechol bound to titanium are currently listed in the Cambridge Structural Database (CSD),[16] only four neutral titanium catecholate structures have been reported.[17,18] On the basis of a survey of the CSD, Gigant et al.[17] identified eight different coordination modes of catechol, several of which occur in the Ti/O clusters described here. In the **Ti_2cat_2** structure, which is a new polymorph of a previously reported structure, the two catechol dianions bind in a bridging chelate μ_2-(O,O′,O′) mode. **Ti_2cat_6** has the largest catechol-to-titanium ratio (3:1) reported for a neutral titanium catecholate to date. The three crystallographically unique catechol ligands, one dianion and two anions, illustrate the variety of ligand binding to TiO clusters. They bind in a singly bridging chelate μ_2-(O,O′,O′) mode, a monodentate mode, and a bidentate mode, respectively, as illustrated in Figure 4. The six unique catechol dianion ligands found in **Ti_6cat_6** are related by a pseudo-C_2 axis, but only two unique modes of binding to the metal centers are present: singly bridging chelate μ_2-(O,O′,O′) (two ligands) and doubly bridging chelate μ_3-(O,O′,O,O′) (four ligands).

Isonicotinic Acid. The reactions between INA and the titanium alkoxides yield more a more consistent binding motif. In all four structures reported herein, INA is deprotonated to give the isonicotinate anion in the single-crystalline phase. It always exhibits monodentate binding of each of the oxygens to a titanium atom, so each ligand bridges two titanium atoms. While no examples of titanium compounds containing INA or its anion could be found in the CSD, four crystal structures of titanium alkoxides containing the related benzoate anion are present. In these structures, the benzoate anion, like the isonicotinate anion, always bridges two titanium centers. It is worth noting that the structure of $Ti_6(\mu_3\text{-O})(\mu_2\text{-benzoato-}O,O')\text{-(2,2-dimethyl-PrO)}$,[19] despite possessing neopentoxide and benzoate instead of isopropoxide and isonicotinate ligands, has the same space group

(14) Redfern, P. C.; Zapol, P.; Curtiss, L. A.; Rajh, T.; Thurnauer, M. C. *J. Phys. Chem. B* **2003**, *107*, 11419–11427.
(15) Grätzel, M. *Inorg. Chem.* **2005**, *44*, 6841–6851.
(16) Allen, F. H. *Acta Crystallogr.* **2002**, *B58*, 380–388.
(17) Gigant, K.; Rammal, A.; Henry, M. *J. Am. Chem. Soc.* **2001**, *123*, 11632–11637.
(18) Davidson, M. G.; Jones, M. D.; Lunn, M. D.; Mahon, M. F. *Inorg. Chem.* **2006**, *45*, 2282–2287.

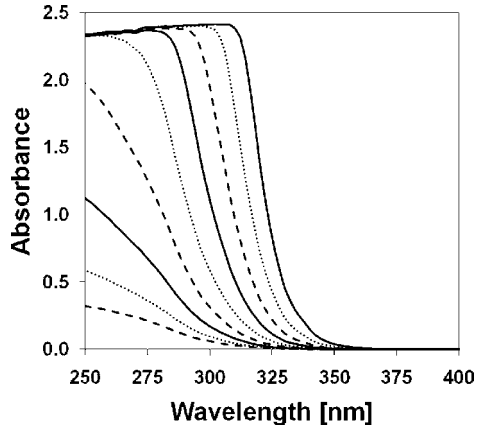

Figure 5. Absorption spectra of $Ti_{17}O_{24}OPr^{i}_{20}$ (**Ti_{17}**) in CH_2Cl_2 at the following concentrations (right to left): 1.3, 0.63, 0.31, 0.16, 7.8×10^{-2}, 3.9×10^{-2}, 2.0×10^{-2}, 9.8×10^{-3}, and 4.9×10^{-3} g/L.

($R\bar{3}$) and molecular packing as **Ti_6INA_6** with identical molecular connectivity of the adsorbents.

Spectroscopic Measurement of the Band Gaps of the Clusters. As described by Adachi,[20] for optical transitions near the absorption edge, the absorption coefficient α (in cm^{-1}) is given by the following expression:

$$\alpha = \frac{B(h\nu - E_g)^n}{h\nu} \quad (1)$$

where B is the absorption constant for the transition, E_g (in eV) is the energy of the band gap, and $h\nu$ (in eV) is the photon energy. The exponent n characterizes the nature of the transition. For allowed direct and indirect transitions (the latter of which also involve momentum transfer), $n = 0.5$ and 2, respectively. For forbidden direct and indirect transitions, $n = 1.5$ and 3, respectively.

Analysis of the absorption coefficient at the onset of absorption for different loading densities has been used to determine the band gap of colloidal anatase nanoparticles,[21] but the analysis was limited to allowed direct or indirect transitions. Absorption spectra of **Ti_{17}** in methylene chloride at concentrations from 4.9×10^{-3} to 1.3 g/L are shown in Figure 5. An increase in baseline absorbance at loading densities greater than 1.3 g/L (not shown in Figure 5) is attributed to scattering from aggregates in solution. At concentrations up to 1.3 g/L, the absorption changes exhibited Beer−Lambert behavior at wavelengths for which the absorbance was below 1.5, indicating that aggregation did not occur at these loading densities.

At the lowest concentration examined (4.9×10^{-3} g/L), the absorption coefficient between 4.4 and 5.0 eV follows a square-root dependence ($n = 0.5$), indicating that this is an allowed direct transition corresponding to a band gap of 4.26 eV ($R^2 = 1.00$). At high loading densities (1.3 g/L), the absorption coefficient at the onset of absorption is best fit by $n = 3$, suggesting that the lowest-energy transition is a forbidden indirect transition with a band gap of 3.36 eV ($R^2 = 0.99$). Fitting the high loading density data using $n = 2$ yielded a nearly identical band gap (3.40 eV), but R^2 was reduced to 0.96.

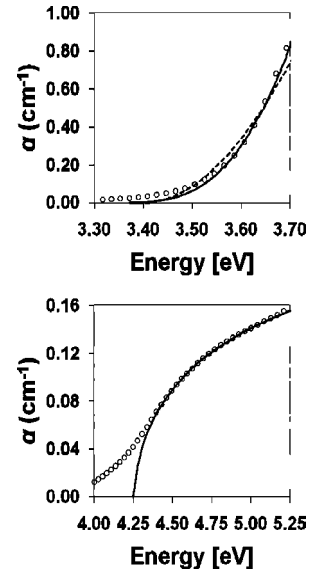

Figure 6. Plots of α (in cm^{-1}) vs photon energy (eV) and corresponding fits to eq 1 for **Ti_{17}** in CH_2Cl_2 with loading densities of (top) 1.3 and (bottom) 4.9×10^{-3} g/L. The top panel shows data (○), the $n = 3$ fit (solid line), and the $n = 2$ fit (dashed line); data (○) and the $n = 0.5$ fit (solid line) are illustrated in the bottom panel.

The experimental and fitted absorption curves of **Ti_{17}** shown in Figure 6 bear a striking resemblence to the curves of colloidal anatase particles with diameters of 2.1, 13.3, and 26.7 nm, as measured by Serpone et al.,[21] which showed a band gap of $E_g = 4.03-4.04$ eV. The band gap of the strongest allowed indirect transition was found to be equal to 3.21 eV. The authors concluded that no size quantization occurred for particles with diameters greater than 2.0 nm. The allowed direct transition across the band gap of ∼4.25 eV in **Ti_{17}** is blue-shifted by ∼0.22 eV relative to that of the anatase nanoparticles.

While our data suggest that the low-energy indirect transition is forbidden rather than allowed, analysis with either function leads to an indirect band gap energy that is ∼0.17 eV larger than the anatase value of Serpone et al.[21]

Theoretical Calculations. Extensive calculations on optimized TiO_2 nanoparticles have been reported by Persson and co-workers.[5,22−24] Density functional theory (DFT) calculations on the experimental structures of the nanoclusters were performed with the Gaussian03 package[25] using the WebMO interface. GaussView[26] was used for visualization and further analysis of the computational results. The hybrid exchange correlation functional B3LYP was used for all of the calculations in the present study. The crystallographic symmetries of the complexes were maintained in all of the calculations. Because of the disorder of the isopropoxide groups in nearly every structure examined, geometry optimizations were performed starting with the crystal structure geometry after removal of a

(19) Ammala, P. S.; Batten, S. R.; Kepert, C. M.; Spiccia, L.; van den Bergen, A. M.; West, B. O. *Inorg. Chim. Acta* **2003**, *353*, 75; CCDC entry 187335.
(20) Adachi, S. *Optical Properties of Crystalline and Amorphous Semiconductors: Materials and Fundamental Principles*; Kluwer: Norwell, MA, 1999; p 280.
(21) Serpone, N.; Lawless, D.; Khairutdinov, R. *J. Phys. Chem.* **1995**, *99*, 16646–16654.
(22) Nilsing, M.; Lunell, S.; Persson, P.; Ojamäe, L. *Surf. Sci.* **2005**, *582*, 49–60.
(23) Persson, P.; Lundqvist, M. J.; Ernstorfer, R.; Goddard, W. A.; Willig, F. *J. Chem. Theory Comput.* **2006**, *2*, 441–451.
(24) Persson, P.; Gebhardt, J. C. M.; Lunell, S. *J. Phys. Chem. B* **2003**, *107*, 3336–3339.
(25) Frisch, M. J.; et al. *Gaussian 03*, revision C.02; Gaussian, Inc.: Wallingford, CT, 2004.
(26) Moser, J.; Punchihewa, S.; Infelta, P. P.; Grätzel, M. *Langmuir* **1991**, *7*, 3012–3018.

Table 1. Calculated HOMO−LUMO Gaps ΔE (eV) of Ligands and Titanium Clusters

	catechol	INA	Ti_2cat_2	Ti_2cat_6	Ti_6cat_6	Ti_3INA_3	Ti_4INA_2	Ti_6INA_6	$Ti_{17}INA_4$	Ti_{17}
symmetry	C_1	C_1	C_1	C_i	C_1	C_1	C_2	C_i	S_4	C_1
E_{LUMO}	−0.29	−2.48	−1.51	−1.90	−1.82	−2.30	−1.99	−2.74	−2.41	−1.93
E_{HOMO}	−6.02	−7.25	−5.29	−5.41	−5.23	−6.93	−6.71	−7.13	−7.02	−6.64
ΔE	5.73	4.77	3.78	3.51	3.41	4.62	4.72	4.39	4.61	4.71

minor disordered component. In the optimized structures, the crystal structure geometry was essentially preserved. The inability to reliably determine the positions of the hydrogen atoms by geometry optimization of the $\mathbf{Ti_{17}cat_4}$ structure prevented its inclusion in the calculations. Final calculations for all of the complexes were completed using the LANL2DZ double-ζ basis set with an ultrafine integration grid. The normalized sum of the squares of the orbital coefficients was used for partitioning the molecular orbitals between the cluster and adsorbates.[5]

Band Structure. The HOMO and LUMO of unsubstituted $\mathbf{Ti_{17}}$ have energies of −6.64 and −1.93 eV, respectively (last column of Table 1), corresponding to a HOMO−LUMO gap ($\Delta E = E_{LUMO} - E_{HOMO}$) of 4.71 eV. B3LYP/VDZ calculations by Lundqvist et al.[5] yielded the slightly larger value of 4.98 eV for an $n_{Ti} = 16$ TiO_2 cluster optimized starting from the structure of anatase. In clusters with adsorbed INA, the HOMO−LUMO gap is only slightly smaller than in $\mathbf{Ti_{17}}$ and varies between 4.4 and 4.7 eV. There is no correlation between cluster size and the calculated band gaps in the limited number of clusters examined in the current study.

The energy of the HOMO−LUMO gap in the titanium clusters with adsorbed catechol (3.41−3.78 eV) is nearly 1 eV smaller than those in $\mathbf{Ti_{17}}$ and the titanium complexes containing INA. In the Ti/catechol complexes, the HOMO, HOMO-1, and HOMO-2 orbitals are localized almost exclusively on the catechol ligand (85−98%), whereas the LUMO, LUMO+1, and LUMO+2 orbitals consist largely of titanium d orbitals (68−72%), indicating that the HOMO-to-LUMO and other low-lying transitions involve catechol-to-cluster charge transfer, in agreement with earlier theoretical calculations of catechol adsorbed on TiO_2.[14] This smaller HOMO−LUMO gap in the Ti/catechol compounds is responsible for their deep-red color. Such coloration is characteristic of catechol adsorbed on anatase nanoparticles, as first reported by Moser and Grätzel[26] and subsequently by numerous others.[13,27,28] The dark-red color observed in all four Ti/catechol complexes presented herein suggests that the number of titanium atoms, or cluster size, has little impact on the size of ΔE, in agreement with the results of our calculations.

On the other hand, the character of the lowest-energy electronic transition in the Ti/INA complexes varies from cluster to cluster. In the $n_{Ti} = 3$ and 6 clusters with INA, the HOMOs consist of 95 and 98% INA orbitals, respectively. For the $\mathbf{Ti_3INA_3}$ cluster, the LUMO is 50% INA- and 41% cluster-centered, so the HOMO−LUMO transition for this compound is a mixture of ligand-to-ligand and ligand-to-cluster charge transfer. The transition is similar for the $\mathbf{Ti_6INA_6}$ cluster, as the LUMO is 64% INA- and 33% cluster-centered. In the $\mathbf{Ti_4INA_2}$ complex, the HOMO is 22% INA- and 30% cluster-centered, with the remainder of the orbital residing on the isopropoxide groups; the LUMO is 72% INA- and 22% cluster-centered. INA contributions are almost completely absent in the $\mathbf{Ti_{17}INA_4}$ HOMO. They account for only 1% of the orbital, whereas 61% of the HOMO is centered on the Ti/O core, with the remainder composed of isopropoxide basis functions. The LUMO is split almost evenly between INA (46%) and the core (52%).

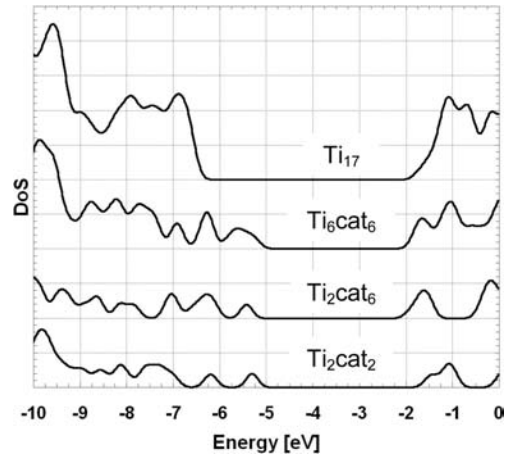

Figure 7. DOS plots for $\mathbf{Ti_{17}}$ and smaller clusters containing catechol, illustrating the band gap and evolution of quasi-valence and -conduction bands with increasing cluster size.

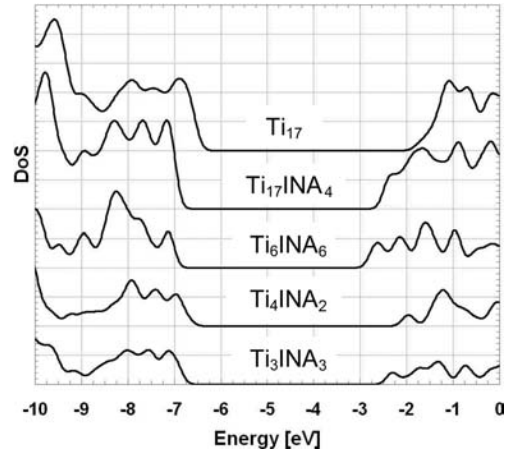

Figure 8. DOS plots of $\mathbf{Ti_{17}}$ and smaller clusters containing INA, illustrating the band gap and evolution of quasi-valence and -conduction bands with increasing cluster size.

While the cluster size seems to have little or no effect on the HOMO−LUMO gap of the titanium cluster, an increase in the size of the cluster is accompanied by the formation of quasi-continuous conduction and valence bands. Density of states (DOS) plots for $\mathbf{Ti_{17}}$ (Figures 7 and 8) reveal the similarity of the pseudoconduction and -valence bands to those of similarly sized anatase particles.[5]

The band gap of ∼4.7 eV calculated for nonfunctionalized $\mathbf{Ti_{17}}$ is larger than our spectroscopic result of ∼4.25 eV. It is well-known that the HOMO−LUMO gap obtained using DFT methods exceeds values calculated using time-dependent DFT.[5]

(27) Wang, Y.; Hang, K.; Anderson, N. A.; Lian, T. *J. Phys. Chem. B* **2003**, *107*, 9434–9440.
(28) Creutz, C.; Chou, M. H. *Inorg. Chem.* **2008**, *47*, 3509–3514.

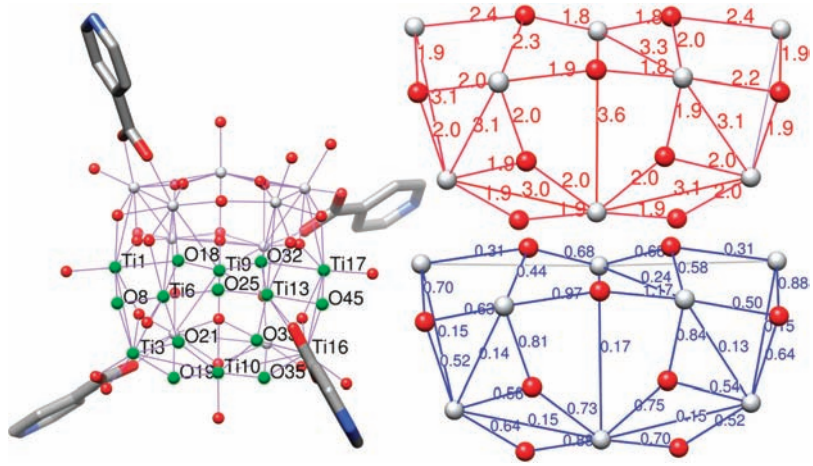

Figure 9. Structure of the $\mathbf{Ti_{17}INA_4}$ complex as optimized using the B3LYP/LANL2DZ method. Independent atoms of the Ti/O core shown in the bond length (upper-right, in Å) and Mayer bond order (lower-right) diagrams are labeled and colored green in the diagram at the left. In the diagrams on the right, the green coloring of the selected atoms has been removed, and the Ti and O atoms are colored silver and red, respectively.

Table 2. Net Charges (*e*) on Free Catecholate and the Adsorbed Catecholate in $\mathbf{Ti_6cat_6}$

bonding	net charge	charges on oxygen atoms
catechol molecule[a]	−1.67	−0.52, −0.47
μ_2-(O,O′,O′)	−1.67	−0.62, −0.70
	−1.72	−0.63, −0.72
	−1.58	−0.63, −0.55
	−1.58	−0.54, −0.63
μ_3-(O,O′,O,O′)	−1.78	−0.69, −0.70
	−1.78	−0.70, −0.71

[a] Hydroxyl hydrogens were omitted in the summation of the atomic charges.

The DOS of clusters containing catechol do not display prominent conduction and valence bands and are instead primarily composed of discrete energy levels. This is not surprising, as the levels between −7 and −5 eV are orbitals of catechol ligands, which are energetically isolated from the remaining cluster orbitals. In the INA clusters, even the smallest, $\mathbf{Ti_3INA_3}$, exhibits a modest conduction band with a significant density of states over a wide energy range. The DOS increases as the number of titanium atoms gets larger. $\mathbf{Ti_6INA_6}$ is the smallest cluster for which a valence-band-type DOS is observed. It grows into a well-formed band in the case of the $\mathbf{Ti_{17}INA_4}$ cluster.

Nature of the Bonding in the Clusters. Analysis of the Mayer bond orders in the clusters shows a significant variation in Ti−O bonding, in agreement with the considerable spread in the Ti−O bond lengths discussed above. The results for $\mathbf{Ti_{17}INA_4}$ are shown in Figure 9. The theoretical and experimental bond lengths agree within ∼0.05 Å (Table S2 in the Supporting Information). Several of the longer bond lengths are overestimated by the calculations. Weak covalency is also found for the Ti−Ti interactions. The covalent contributions to the cluster's stability are clearly considerable. The calculations do not show significant charge transfer from the catechol into the cluster in the ground state, as shown for $\mathbf{Ti_6cat_6}$ in Table 2.

The negative charges on the catecholate adsorbent are similar to those in the isolated cation but larger for the μ_3-(O,O′,O,O′) bonding mode. The oxygen atoms are more negative in this bonding mode, in which each oxygen is linked to two Ti atoms (Figure 4). Unlike earlier studies,[29] the calculations showed no evidence for a significant enhancement of the dipole moment upon adsorption.

Conclusions

While research involving wide-band-gap semiconductor particles has attracted considerable attention, the lack of atomic-resolution structures of the nanoparticles or adsorbed dye sensitizers introduces ambiguities into the structure/function relationships. The crystalline phase of nanoparticles functionalized with technologically relevant ligands offers the opportunity to obtain unambiguous structural information. The particles can be synthesized and subsequently self-assembled into single crystals suitable for structure determination, spectroscopic characterization, and theoretical analysis. The UV−vis spectra of the Ti_{17} nanoparticles presented herein are remarkably similar to those of semiconductor nanoparticles currently employed in photovoltaic research. The band gaps of the Ti_{17} cluster derived from the spectra and the theoretical calculations agree within a few tens of electron volts with that measured for anatase. The Ti−O bond lengths in the clusters show a larger range than those in the known TiO_2 phases, indicating the importance of surface effects. The catecholate adsorbent exhibits four different modes of binding to the clusters. The effect of such differences on physical properties merits further attention.

Acknowledgment. This work was funded by the Division of Chemical Sciences, Geosciences, and Biosciences, Office of Basic Energy Sciences, of the U.S. Department of Energy through Grant DE-FG02-02ER15372. Technical assistance by Renata Freindorf is greatly appreciated.

Supporting Information Available: Complete ref 25, Tables S1 and S2, and crystallographic data for the clusters (CIF). This material is available free of charge via the Internet at http://pubs.acs.org.

JA909600W

(29) Rajh, T.; Chen, L. X.; Lukas, K.; Liu, T.; Thurnauer, M. C.; Tiede, D. M. *J. Phys. Chem. B* **2002**, *106*, 10543–10552.